2016

CFD Approaches Applied To A Single-Screw Expander

Davide Ziviani
Ghent University, Belgium, davide.ziviani@ugent.be

Alessio Suman
University of Ferrara, alessio.suman@unife.it

Jacopo Gabrielloni
University of Ferrara, jacopo.gabrielloni@student.unife.it

Michele Pinelli
University of Ferrara, michele.pinelli@unife.it

Michel De Paepe
Ghent University, Belgium, michel.depaepe@ugent.be

See next page for additional authors

Authors
Davide Ziviani, Alessio Suman, Jacopo Gabrielloni, Michele Pinelli, Michel De Paepe, and Martijn van den Broek

CFD Approaches Applied To A Single-Screw Expander

Davide ZIVIANI[1]*, Alessio SUMAN[2], Jacopo GABRIELLONI[2], Michele PINELLI[2], Michel DE PAEPE[1], Martijn VAN DEN BROEK[1]

[1]Ghent University, Department of Flow, Heat and Combustion Mechanics, Ghent, Belgium
davide.ziviani@ugent.be, michel.depaepe@ugent.be, martijn.vandenbroek@ugent.be

[2]Engineering Department in Ferrara, University of Ferrara, Ferrara, Italy
alessio.suman@unife.it, jacopo.gabrielloni@student.unife.it, michele.pinelli@unife.it

* Corresponding Author

ABSTRACT

Organic Rankine Cycle (ORC) systems rely on the expander performance to generate power output in an efficient manner. Especially in the low power range (below 100 kWe), positive displacement (PD) expanders (e.g. scroll, twin-screw, reciprocating, vane, spool, etc.) result to be cost-effective. However, commercially available PD expanders are still limited and, in many cases, the existing PD compressors are operated in reversed mode by introducing design modifications to sealing, bearings, port sizes, lubrication requirements to increase both their performance and reliability. Computational fluid dynamics (CFD) as a design and analysis tool of positive displacement machine has been proven to be viable. Challenges arise when CFD is applied to PD machines due to the dynamics of the expansion (or compression) process, presence of internal leakages and heat transfer mechanisms, as well as deforming working chambers. Different grid generation methods and solution schemes have been successfully implemented to scroll, twin-screw and reciprocating machines (Rane *et al.*, 2012, Rane *et al.*, 2013). The limitation of such methodologies to be applied directly to complex multi-rotor machines has been highlighted by Rane et al. (Rane *et al.*, 2012). In this paper, a single-screw expander is used as benchmark to evaluate different grid generation methodologies (dynamic remeshing and Chimera strategy overlapping grid) and commercial software, in terms of computational resources required, accuracy of the results and limitations. The calculations have been performed with air to reduce the complexity of the problem.

1. INTRODUCTION

Organic Rankine Cycle (ORC) is a proven technology to convert waste heat from several sources and in a wide range of power outputs (Quoilin *et al.*, 2013). Especially in the medium to low power range, volumetric expanders play an important role because of their performance and lower investment costs compared to dynamic expanders (Imran *et al.*, 2016). As a consequence, the efficiency of the expander represents a key parameter to be optimized in order to maximize the power output. Different types of positive displacement machines, such as scroll or twin screw, have been investigated for their use in ORCs. Recently the single screw expander (SSE) is gaining interest as a potential volumetric expander for ORC applications. Similarly to a twin screw expander, the single screw is generated by two meshing profiles: a grooved central rotor engages with the lateral toothed satellites (or gaterotors). The meshing between each groove with the corresponding tooth isolates a working chamber, i.e. a portion of the groove. In comparison with the twin screw, the SSE has longer bearings life due to balanced loading on the main rotor, high volumetric efficiency, low leakage, low noise and vibration and a simplified configuration (Ziviani *et al.*, 2014a). The design of ORC systems requires also the selection of a suitable working fluid. Screening methods have been developed to identify optimal working fluids by taking into account environmental and safety criteria along with thermophysical properties (Saleh *et al.*, 2007). However, using real gas properties in CFD simulations is still a challenging quest due to high computational cost and convergence issues. To the Author best knowledge, CFD analyses applied to single screw machines are rare due to the complexity of the problem especially regarding the mesh generation. The aim of this paper is to evaluate and compare different meshing techniques and solution schemes when applied to a single screw geometry. Pros and cons of commercial software are discussed and the accuracy of the results is analyzed by comparing the results obtained with each of them. Both steady-state and transient analyses have been investigated.

2. SINGLE-SCREW EXPANDER GEOMETRY AND BOUNDARY CONDITIONS

The single-screw expander considered as case study is an 11 kWe air-compressor adapted to be an expander for organic Rankine cycle (ORC) applications. The details of the main dimensions of the expander are listed in (Ziviani *et al.*, 2016). However, the real geometry has been simplified accordingly in order to perform CFD analyses. In particular, the main rotor shaft and its sealing have been removed as well as the bearings. Similar modifications have been applied to the starwheels. Instead, the housing has been kept in its original form to accurately predict the internal flows and the 3D CAD geometry is shown in Figure 1. The same boundary conditions have been applied for each simulation, i.e. an inlet pressure of 1200 kPa, an inlet temperature of 390 K, and an outlet pressure of 200 kPa. The chosen working fluid was air to simplify the analysis, and the equation of state (EOS) used the ideal gas law. The standard turbulence model k-ε combined with standard wall functions was used. This model has proven to be, also in this case, the best compromise between accuracy, robustness and computational effort. The main rotor has a rotation speed of 3000 rpm, while the rotational speed of satellites have been obtained by considering the 6/11 engaging ratio between grooves and teeth.

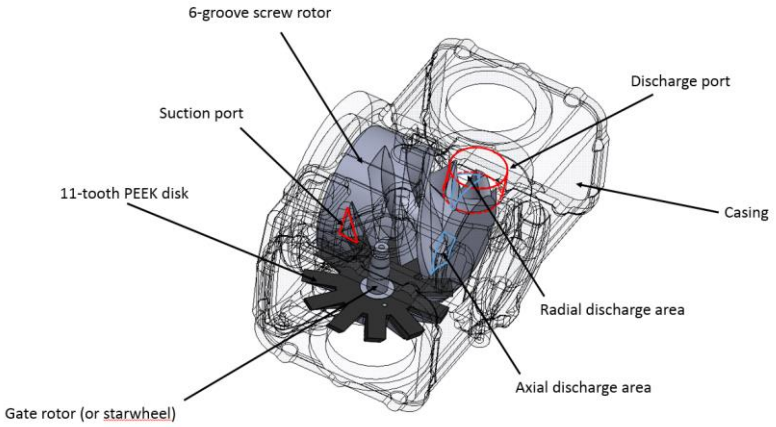

Figure 1: Single-screw expander geometry.

3. MESHING TECHNIQUES

The aim of this section is to evaluate and compare four different meshing techniques applied to a single-screw expander. Since the analyzed methodologies are not available in a single software, each technique is associated to a specific software. The meshing methods and the specific software used (in brackets) are as follows: (i) Dynamic Mesh (DM) (ANSYS Fluent 13.0); (ii) Chimera Strategy (CS) (CD-ADAPCO STAR-CCM+ 10.02); (iii) Mesh Morphing (MM) (PumpLinx 4.0.3); (iv) Key-Frame Re-meshing (KFR) (ANSYS CFX 15.0).

3.1 Dynamic Mesh

By using the DM strategy implemented in ANSYS Fluent 13.0, the mesh inside the screw and satellites profiles is regenerated at each time step to accommodate the shape and size change of the gas pockets. The mesh regeneration could follow element size criteria and/or element quality criteria (such as skweness). The numerical domain of the single-screw expander is discretized through the use of a triangular mesh. In order to to increase the resolution of the mesh close to the walls, a local mesh refining approach has to be adopted. Figure 2 highlights the grid deformations during the rotation of main rotor and corresponding gaterotor. In the flank gap there are at least two triangular mesh elements in agreement with the data reported in literature (Castilla *et al.*, 2010 and Del Campo *et al.*, 2012) for positive displacement machines. One of the CFD simulation was carried out as a steady-state numerical model by using a DM strategy implemented in ANSYS Fluent 13.0. Eventually, a transient analysis is able to reproduce the real operation of the machine through a sequence of relative positions between the central screw and the satellites by imposing an angular increment. For example, the use of 2D CFD analysis by using a DM for studying some particular fluid dynamic phenomena in the gear pumps. In particular, Castilla *et al.* (2010) put the attention to the turbulence structure in the suction chamber, while Del Campo *et al.* (2012) analyzed pressure variations and

cavitation phenomena. In these cases, the 2D strategy allows the comprehension of the major fluid dynamic phenomena involved.

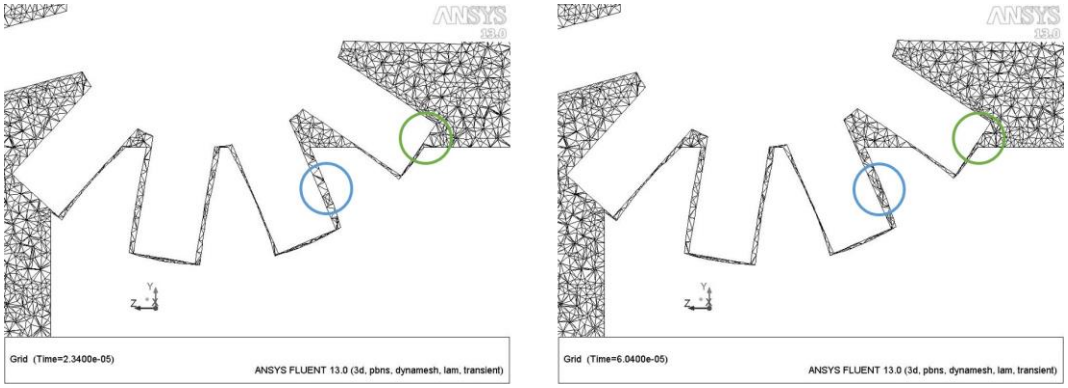

Figure 2: Dynamic tetrahedral mesh evolution through time.

3.2 Chimera Strategy

Overlapping grid, subsequently named the Chimera approach, was first introduced in the early 1980's (Steger and Benek, 1987) when several grid assembly packages have become available (Roget and Sitaraman, 2014). In the present paper, the simulation of the scroll expander with the CS was carried out by means of CD-ADAPCO STAR-CCM+ 10.02. The overset method consist in the contemporary use of active cells and passive cells. In active cells, regular discretized equations are solved, while in passive cells, no equation is solved, they are temporarily or permanently de-activated. Active cells along interface to passive cells refer to donor cells at another grid instead of the passive neighbors on the same grid. The first layer of passive cells next to active cells are called acceptor cells. The solution is computed on all grids simultaneously. Grids are implicitly coupled through the linear equation system matrix. Different interpolation functions can be used to express values at acceptor cells via values at donor cells. The donor cells must be active cells, and the change of cell status is automatically controlled by the solver. Overset grids usually involve one background mesh, which is adapted to environment, and one or more overset grids attached to bodies, overlapping the background mesh and/or each other as reported in Figure 3. Each grid (background and overset) can move according to the motion models implemented in the CFD software. In literature, the comparison between the CS and other CFD strategies are limited. Togasci *et al.*, 2001 and Hoke *et al.*, 2009 report the applications of the overset grid for a rocket booster and a 2D airfoil, respectively. Comparison with experimental data (Togasci *et al.*, 2001) and other CFD solutions (Hoke *et al.*, 2009) demonstrated that the CS is reliable for different fluid dynamics applications. The major difference with respect to the DM approach consists that CS does not deform the mesh during the calculation.

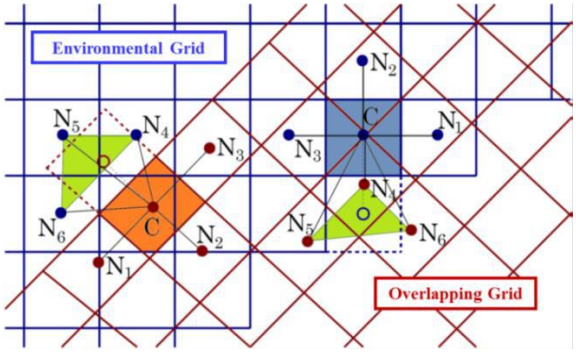

Figure 3: N_1, N_2, N_3 neighbors from the same grid; N_4, N_5, N_6 neighbors from overlapping grid (adapted from Schreck and Peric, 2012).

In the present paper the background mesh and the three overlapping mesh are reported in Figure 4. In this case, each overlapping grid has to interface with the background mesh, moreover there are two additional overset interfaces

between each satellite and the central screw. For this particular configuration, the central screw is considered as the background for the two satellites. To obtain a good interface quality, local refinements have been done in the background mesh to lower cell dimensions in the overlapping zone and reasonably increase the element number. Overlapping meshes are made of 5,033,265 elements (839,113 for the screw and 2,097,068 for each satellite), while the background mesh consists of 3,210,621 elements. Overlapping and background mesh are constitute by Cartesian elements and prism layer close to the wall.

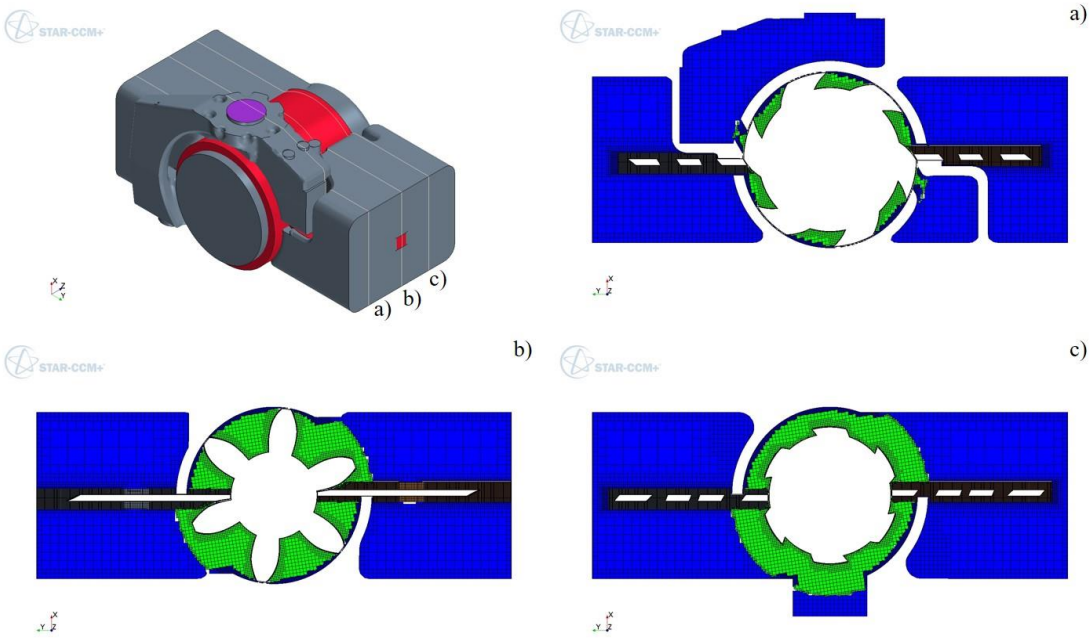

Figure 4: Chimera geometry and planar section at a) inlet ports b) center of the device c) outlet port. It is possible to see the background region (blue) and the overlapping ones (yellow for the screw, grey and orange for the starwheels).

As said before, the presence of three rotating regions implies the presence of three overset mesh boundaries. Moreover, as the gaterotor regions have to communicate between the background and the screw, the number of overset interfaces increases up to five (the three canonical between each rotating region and the background, and the two interfaces between the screw and the gaterotors). This number of interfaces is easily handled by the software, however it is possible that this could lead to higher solution time.

3.3 Mesh Morphing

Metamorphosis (or Morphing) is the process of gradually changing a source object through intermediate objects into a target object (Lee *et al.*, 1999). Morphing a mesh to be used in a numerical simulation is a delicate task, especially for a 3D CFD mesh. In this case, the morphing, also termed smoothing, is not limited to the surface but has to be extended to the entire volume of the mesh and the solver suffers dramatically.. The way the task is accomplished, depends on which smoothing algorithm is selected and on the definition of the control points criteria which can substantially change the result. A key feature that can be used to subdivide them is how they are related to the original mesh. The software in which mesh morphing is implemented and that is used in this paper is PumpLinx. Pumplinx has the capability of meshing pumps, gears and compressors by using this technique under the form of preloaded templates. In particular, the SCORG module has been designed for screw compressors and adapted to screw expanders in this paper. SCORG is a software for the design and analysis of screw compressors, pumps and rotors. The actual limit is given by the number of screw rotors that the SCORG module can deal with. In fact, only compressors with two or more screw rotors can be meshed with this template, which makes it unusable for a SSE application. This method, due to the combination of structured mesh and prescribed motion, sounds to be the best approach to this kind of application. However, as it is not possible to fit the SCORG module to SSE (Kovacevic *et al.*, 2012), at the moment the best compromise is given by the CS.

3.4 Key-frame re-meshing

Key-frame remeshing (KFR) is a meshing method where, after each time step, the volume is checked to see if cell's quality is still good to absorb further deformation without generating negative volume elements. If not, some group of cells are locally remeshed (Rane et al., 2012). This implies that number and connectivity of the cells changes from one step to another. It has been demonstrated that this meshing technique could simulate the complex configuration of screw compressors, however at the moment there are many limitations on pre-processing time, computational resources, results accuracy and difficulties in including features like turbulence or multiphase flows. Two tests were conducted on a piston cylinder and a twin screw compressor (Kovacevic *et al.*, 2012). In the piston cylinder application, significant errors in the prediction of pressure and temperature are present, while all attempts made with a twin screw compressor failed due to the complexity of numerical mesh. The analysis made on the piston gave important information on the level of accuracy of the KFR, with the error that increases with grid refinement. This could be due to mesh replacement at each time step, which means that it is possible that space conservation is violated with KFR. In conclusion, KFR gives inconsistent results, with an error that increases with mesh refinement instead of becoming smaller (Rane *et al.*, 2013). Time step reduction made excessive demands on pre-processing, making this path not suitable at this time.

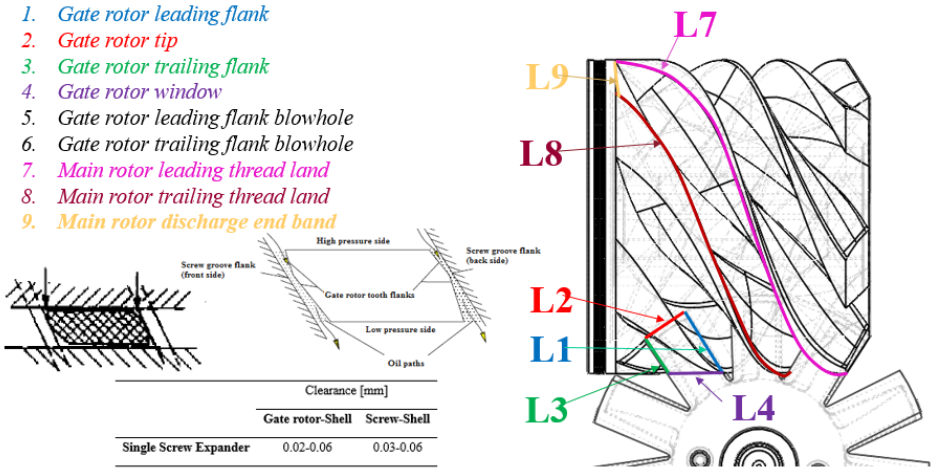

Figure 5: Possible leakage paths in single screw compressors and expanders (Adapted from Ziviani *et al.*, 2014a).

4. SIMULATION ANALYSIS

The prepared simulations were performed under steady-state conditions, with the exception of the CS one which was performed also under transient conditions. Each approach can provide different insights and useful information. The steady-state simulation is useful to evaluate the volumetric efficiency, axial thrusts and therefore a preliminary structural analysis. Moreover, the steady-state approach allows to calculate the flow coefficients (C_d) of the gaps which relates the flow rate through the machine and the pressure drop across the gaps. This is very useful to tune lumped parameter models, where gap flow coefficients are fundamental to improve the model accuracy on the mass flow predictions. At the same time, they are very difficult to be estimated by means of experimental data and/or analytical/empirical relations. For these reasons, CFD models (even steady-state) are increasingly used to determine these crucial coefficients. However, the transient simulation, besides the allows to evaluate the evolution-in-time of parameters of interest such as flow rate, pressure and torque. Since the SSE is a positive displacement machine, its volumetric efficiency is heavily affected by different kind of leakage paths (Ziviani *et al.*, 2014a). The most common leakage paths are shown in Figure 5. In particular, a total of nine sealing lines can be identified: L1 and L3 are related to the gaps which exist between the screw and satellite tooth tip and flank; L2 is satellite tooth tip (its presence is connected to the manufacturing process, i.e. milling); L4 is the gap between housing and screw and it is necessary to permit the screw motion; L7 and L8 are screw leading and trailing edges; L9 is the end curved edge of the groove (even this gap is with the housing); while L5 and L6 are blowholes which existence is due to the imperfect shape of satellite teeth. Both steady and transient simulations consider these leakage paths.

4.1 Steady-state approach

Generally, meshing strategies are useful to simulate moving and deforming fluid domains but at the same time also the computational time required increases. Therefore, in the case of steady-state simulations such approaches are not required.

Each steady-state simulation has been run on a Cartesian grid with slight differences on the grid topology among different solvers. The PumpLinx General Mesher did not allow to set prism layers around the wall boundaries, while the meshes generated in STAR-CCM+, Ansys Fluent and CFX did have the possibility to fully define the prism layers at the walls. In terms of number of elements, the mesh generated in PumpLinx, STAR-CCM+, Fluent and CFX consisted of about 500000, 1500000, 3000000 and 2800000 elements, respectively.

4.2 Transient approach

The transient simulation was performed only by means of the CS implemented in CD-ADAPCO STAR-CCM+ 10.02. Boundary conditions were kept the same, expect for the addition of the time step set to 10^{-4} s. The details of the mesh have been outlined in Section 3.2. For completeness, it is mentioned that all the meshing methods supported by the other software were tested. However, the different tests showed that KFR was not able to converge during early stages of the simulation. MM did not allow for transient simulation and DM required extremely high computational resources.

5. RESULTS

5.1 Steady-state approach results

The results presented in the following are related to the C_d obtained in the four different simulations and are aimed at comparing the different approaches. The C_d is an index which, combined to the volumetric efficiency, can give information on the losses and on the leakage flows which occur in a positive displacement device. It is defined as follows:

$$C_d = \frac{Q}{A\sqrt{\frac{2\Delta p}{\rho}}} \tag{1}$$

where Q is the volumetric flow rare [m^3/s], A is the passage area [m^2], Δp is the pressure drop [Pa] between two sections conveniently chosen upstream and downstream the passage area and ρ [kg/m^3] is the fluid density. The higher this value is, the higher are the losses due to leakage flow. To calculate this factor it is necessary to fix a section of known area A, across which the volumetric flux Q can be calculated by means of CFD simulations, and two arbitrary planes where it is possible to calculate the average pressure and, hence, the pressure drop. Figure 6 shows the section positions, referring to the simulation ran in STAR-CCM+. The calculations performed by means of the other methods rely on the same planes.

Table 1: Comparison between the C_d given by the steady simulations.

Software	C_d – Starwheel 1	C_d – Starwheel 2
Ansys Fluent 13.0	0.402	0.488
Ansys CFX 15.0	0.399	0.463
CD-ADAPCO STAR-CCM+ 10.02	0.402	0.497
PumpLinx 4.0.3	0.364	0.439

The results are reported in Table 1. As can be seen, the C_d values for both Satellite 1 and Satellite 2 are of the same order of magnitude with a maximum difference of about 10%. Moreover, since Satellite 1 has a shorter duct, it was expected that the calculated Cd would be smaller than Satellite 2. The first three calculations surprisingly predicted C_d values in close agreement each other (less than 1% difference). Only the fourth calculation deviates from the other of about 10%. In the case of Satellite 2, almost the same behavior is noticed: the first three calculations predicted C_d values within a 5% difference, while the fourth deviates of about 10%. This behavior could have an explanation by considering that Pumplinx is optimized for transient calculations, and in particular the grid topology is conceived to meet this task. Nevertheless, also this software allowed the obtainment of C_d values which can be considered to achieve an enhanced information with respect to usual practice. As for computational resources, PumpLinx, in

particular due to the coarser mesh, reached convergence in less than 1500 iterations and less than an hour. STAR-CCM+ reached convergence in 2000 iterations and some hours of simulation run, while Fluent could not reach convergence before 70000 iterations and 15 days of running simulation. CFX has an intermediate solution time of 15000 iterations and 2 days.

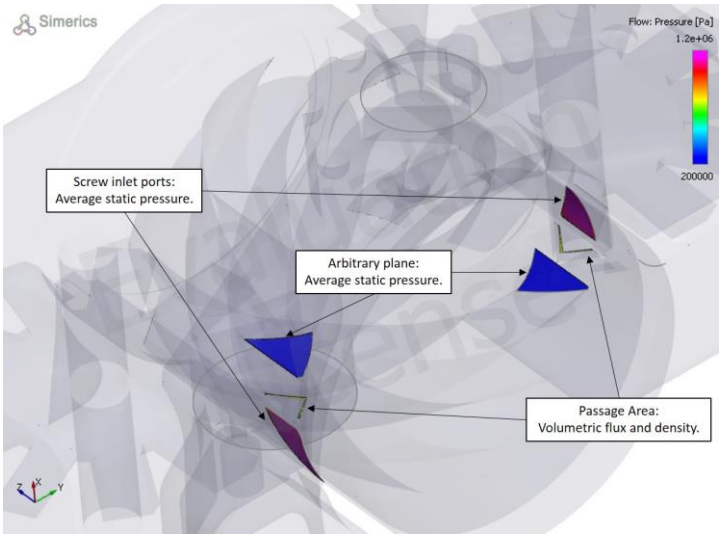

Figure 6: Surfaces employed for the calculation of flow coefficients C_d.

5.2 Transient approach results

A transient analysis provides insights on the dynamic behavior of the expander. As this work presents preliminary results of CFD simulations on a single-screw expander, particular attention is given to verify the reliability of the results obtained. In particular, the inlet and outlet pressure and mass flow rate fluctuations are considered along with the torque generated at the main rotor shaft. Moreover, pressure fluctuations have also been monitored at the screw-expander triangular inlet port closest to the main inlet. The different variables of interest are plotted as a function of the normalized angular position of the screw. The mean values over one full rotation are then compared with the results obtained from the deterministic model (Ziviani *et al*. 2016).

In Figure 7, it is possible to notice the three working chambers that are isolated by the gaterotors on the central screw. As expected, the gaterotors create three sections on the groove, lowering the pressure from the inlet to the discharge pocket. The contour of the pressure is overlaid on the main rotor.

Pressure signals have been monitored circumferentially along the rotor to reconstruct the pressure traces in the grooves. In Figure 8, the main pressure signals are plotted for one revolution. As there are six grooves in the main rotor, six peaks can be identified in the plot.

The 3D CFD model allows to investigate the flow distribution inside the inlet duct. The pressure fluctuations at the triangular inlet ports are shown in Figure 9. The fluctuations present different trends suggesting that the inlet duct induces pressure waves and pressure drops. Such effects cannot be captured by the deterministic model without a coupling with a pressure pulsation model. The pressure fluctuations have direct influence of the mass flow rate as reported in Figure 10a. In fact, each peak of the mass flow rate corresponds to a valley in inlet pressure trend. This behavior can be clearly seen in Figure 10b, where static, dynamic and total pressure traces are overlaid.

The expanding working fluid generates a mechanical torque and therefore produces useful mechanical work. From the CFD model it is possible to extract the actual mechanical torque that can be directly compared to experimental measurements if available. As shown in Figure 8, the value of the shaft torque varies in the range from 12 Nm to 35 Nm, with a mean value of 25 Nm, giving an output power of 7.8 kW (mean value) at 3000 rpm. However, from the deterministic model, the maximum shaft power obtained was in the order of 9 kW. This difference could be given by the presence of enlarged gaps, to help the overset mesh coupling. Similar values were also measured by running the expander with R245fa.

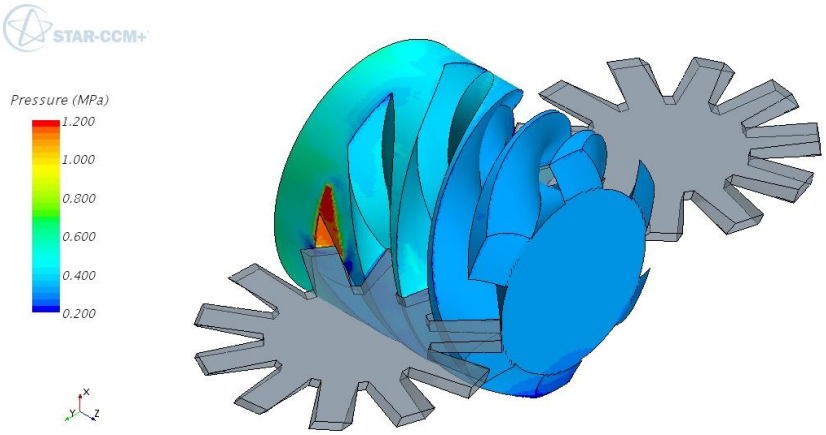

Figure 7: Different working chambers (i.e. portion of the grooves) isolated by the gaterotors.

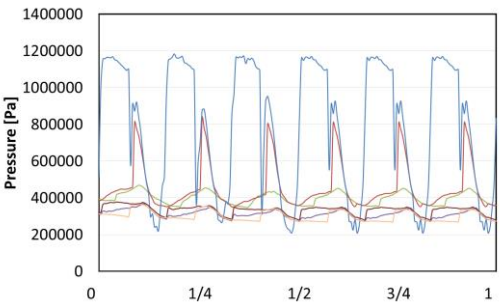

Figure 8: Pressure traces at main screw rotor.

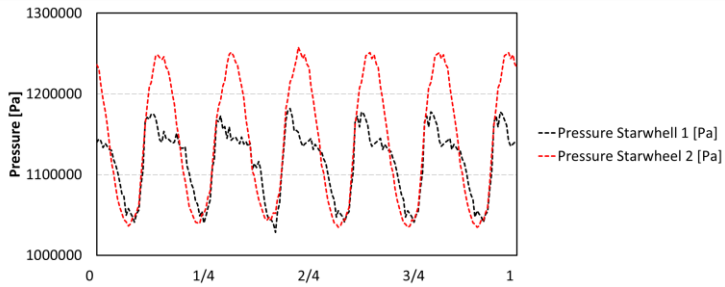

Figure 9: Pressure fluctuations at the main rotor triangular ports.

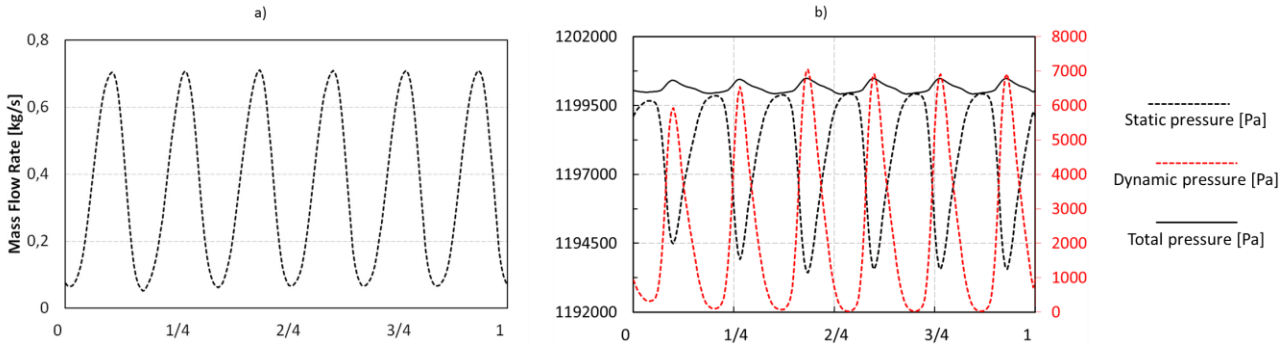

Figure 10: Inlet a) mass flow rate and b) pressure trends.

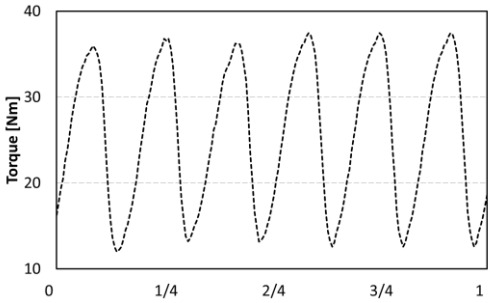

Figure 11: Shaft torque (main screw rotor).

6. CONCLUSIONS

Different CFD approaches applied to a SSE are compared in this paper, both in steady-state and transient conditions. Different commercial software has been considered in order to identify the most suitable to simulate the SSE. All the evaluated software could perform a steady-state simulation to estimate the flow coefficients and a maximum deviation of 10% was obtained, which can be considered acceptable. Among the investigated methods, the transient simulation could be run successfully only with CS. The fluid domain generated by the meshing of screw rotor and two starwheels makes the interpolation between overset and background regions critical and information is lost during the interpolation especially in regions such as gaps between screw and satellites. From the preliminary CFD results it can be concluded that CS showed some potential as meshing strategy for single-screw type of machines. However, in order to improve the converge of the solution further work is required to investigate the influence of meshing parameters as well as the time-step taken.

NOMENCLATURE

Variable	Definition	Units
Q	Volumetric flow rate	[m^3/s]
m	Mass flow rate	[kg/s]
ρ	Density	[kg/m^3]
Δp	Pressure drop	[Pa]
p_{tot}	Total pressure	[Pa]
p_{stat}	Static pressure	[Pa]
A	Passage area	[m^2]
SSE	Single-screw expander	
PD	Positive displacement	
DM	Dynamic Mesh	
CS	Chimera strategy	
MM	Mesh morphing	
SCORG	Screw compressor rotor grid generator	
KFR	Key-frame re-meshing	

REFERENCES

Castilla, R., Gamez-Montero, P. J., Ertürk, N., Vernet, A., Coussirat, M., Codina, E., 2010, Numerical simulation of turbulent flow in the suction chamber of a gear pump using deforming mesh and mesh replacement, Int. J. Mech. Sci., 52, pp. 1334-1342.

Del Campo, D., Castilla, R., Raush, G. A., Gamez-Montero, P. J., Codina, E., 2012, Numerical Analysis of External Gear Pumps Including Cavitation, J. Fluids Eng., 134, p. 081105.

Hoke, C., Decker, R., Cummings, R., McDaniel, D., Morton, S., 2009, Comparison of Overset Grid Deformation Techniques Applied to 2-Dimensional NACA Airfoils, 19th AIAA Computational Fluid Dynamics Conference, 22 - 25 June 2009, San Antonio, Texas, US.

Imran, M., Usman, M., Park B-S, Lee, D.-H., 2016, Volumetric expander for low grade heat and waste heat recovery applications, Renewable and Sustainable Energy Reviews, *57*, 1090-1109

Lee A., Dobkin D., Sweldens W., Schroder P., "Multiresolution Mesh Morphing" (1999), Proceedings of SIGGRAPH 99. Pp. 343-350.

Quoilin, S., van den Broek, M., Declaye, S., Dewallef, P., Lemort, V., 2013, Techno-economic survey of Organic Rankine Cycle (ORC) systems, Renewable and Sustainable Energy Reviews, 2013, *22*, 168-186

Rane S., Kovacevic A., Kethidi M., "CFD Modeling in Screw Compressors with complex multi rotor configurations"(2012), Int. Compressor Engineering Conference at Purdue Univ. Paper 2141.

Rane S., Kovacevic A., Stosic N., Kethidi M., "Grid deformation strategies for CFD analysis of screw compressors", Int. J. Refrigeration, 36(2013), 1883-1893.

Roget, B., Sitaraman, J., 2014, Robust and efficient overset grid assembly for partitioned unstructured meshes, J. Comput. Phys., 260, pp. 1-24.

Saleh, B., Koglbauer, G., Wendland, M., Fischer, J., 2007, Working fluids for low temperature organic Rankine cycles, Energy, 2007, *32*, 1210-1221

Schreck, E., Peric, M., 2012, Overset Grids in STAR-CCM+: Methodology, Applications and Future Developments, STAR Japanese Conference 2012.

Steger, J. L., Benek, J. A., 1987, On the use of composite grid schemes in computational aerodynamics, *Computer Methods Appl. Mech. Eng.*, 64, pp. 301–320.

Togashi, F., Nakahashi, K., Ito, Y., Iwamiya, T., Shimbo Y., 2001, Flow Simulation of NAL Experimental Supersonic Airplane/Booster Separation Using Overset Unstructured Grids, Comput. Fluids, 30(6), pp. 673-688.

Ziviani, D., Bell, I., De Paepe, M., van den Broek, M., 2014a, Comprehensive Model of a Single Screw Expander for ORC-Systems, 22nd International Compressor Engineering Conference at Purdue, Purdue, 14 - 17 July, 2014, Paper n. 1506, pp. 1-10.

Ziviani, D., Suman, A., Lecompt, S., De Paepe, M., van den Broek, M., Spina, P. R., Pinelli, M., Venturini, M., Beyene, A., 2014b, Comparison of a Single-Screw and a Scroll Expander under Part-Load Conditions for Low-Grade Heat Recovery ORC Systems, Proc. of 6th International Conference on Applied Energy (ICAE2014), Taipei, 30 May - 2 June, 2014, Paper n. 78, pp. 1-4.

Ziviani, D., Bell, I., De Paepe, M., van den Broek, M., 2016, Mechanistic model of an oil-flooded single-screw expander, 23rd International Compressor Engineering Conference at Purdue, Purdue, 11 - 14 July, 2016, Paper n. 1486, pp. 1-10.